VOL. 9, NO. 12, DECEMBER 2014 ISSN 1819-6608
ARPN Journal of Engineering and Applied Sciences


www.arpnjournals.com

PRESSURE AND PRESSURE DERIVATIVE ANALYSIS FOR FRACTURED HORIZONTAL WELLS IN UNCONVENTIONAL SHALE RESERVOIRS USING DUAL-POROSITY MODELS IN THE STIMULED RESERVOIR VOLUME

Freddy Humberto Escobar[1], Karla María Bernal[1] and Guiber Olaya-Marin[2]
[1]Universidad Surcolombiana/CENIGAA, Avenida Pastrana, Neiva, Huila, Colombia
[2]Universidad Surcolombiana, Avenida Pastrana, Neiva, Huila, Colombia
E-Mail: fescobar@usco.edu.co

ABSTRACT

Nowadays, the oil industry efforts revolve around the exploitation of hydrocarbon-bearing shale formations. At the current rate of exploitation several shale formations can produce for more than 200 hundred years. Therefore, researches are conducted for a better characterization of these formations so all the local details can be captured by the mathematical models. From the well test point of view, some mathematical models to observe transient pressure behavior have been introduced. However, such models are very complex and may not be practical for a practicing engineering who neither does have the time to code such models or their computer programming capabilities are not good enough. Then, this work takes two mathematical models from the literature as the basis to develop a practical well test interpretation methodology using characteristic points found of the pressure and pressure derivative curves. The resulting methodology was successfully tested with synthetic examples.

Keywords: pseudosteady state, bilinear flow regime, transient-pressure analysis, shale.

1. INTRODUCTION

Currently, pressure transient analysis is focused on the characterization of such unconventional systems as shale formations which permeability is extremely low going to the range of microdarcies to nanodarcies.

The mathematical model governing either rate- or pressure-transient behavior are complex and none of the commercial well test interpretation softwares have included them. Then, there is a need of providing practical interpretation techniques as those presented by Bernal, Escobar, and Ghisays-Ruiz (2014) and Escobar, Montenegro, and Bernal (2014) who used the philosophy of the *TDS* technique, Tiab (1993), for the development of easy-to-use interpretation methodology.

The models proposed by Brown *et al.* (2011) allows to study the well-pressure behavior of shale formations using the stimulated reservoir volume, SRV, concept around a horizontal well and divided into three different zones which have individual properties. The first one corresponds to the finite-conductivity hydraulic fracture. The second zone deals with the inner reservoir region which can be either homogeneous or naturally fractured, and the third one deals with the external portion. Brown *et al.* (2011) consider that the naturally fracture reservoir can be governed by a pseudosteady-state or transient model; then, two models were developed by them and use in this work to provide an interpretation methodology using characteristic points found on the pressure derivative plot. The developed equations were successfully tested with simulated cases.

2. MATHEMATICAL FORMULATION

2.1. Mathematical model

This study is based on the solutions of the trilinear-flow model for pressure-transient responses of fractured horizontal wells in unconventional shale reservoirs presented by Brown *et al.* (2011) who developed their solutions following the work of Cinco-Ley and Meng (1988) for the finite-conductivity fracture solution in a dual-porosity reservoir. Brown *et al.* (2011) derived their solution for the outer reservoir, inner reservoir, and the hydraulic fracture, and then couple the solutions with the flux- and pressure- continuity conditions on the interfaces between the regions and then inverted numerically from the Laplace space. Their mathematical model is brought here and given below.

Outer reservoir solution

The outer reservoir solution in the Laplace space is given by:

$$\bar{P}_{OD}\big|_{x_D=1} = \bar{P}_{ID}\big|_{x_D=1} \cdot \frac{\cosh\left[\sqrt{\sqrt{s/\eta_{OD}}}\,(x_{eD}-x_D)\right]}{\cosh\left[\sqrt{\sqrt{s/\eta_{OD}}}\,(x_{eD}-1)\right]} \quad (1)$$

The outer reservoir solution, P_{OD}, is given in terms of the inner-reservoir pressure at the interface of the inner and outer reservoir pressure at the interface of the inner and outer reservoirs, $\bar{P}_{ID}\big|_{x_D=1}$.

Inner-reservoir solution

The solution for this case in the Laplace space is:

$$\bar{P}_{ID} = (\bar{P}_{FD}\big|_{y_D = w_D/2}) \left(\frac{\cosh\left[\sqrt{\alpha_o}(y_{eD} - y_D)\right]}{\cosh\left[\sqrt{\alpha_o}(y_{eD} - \frac{w_D}{2})\right]} \right) \quad (2)$$

Where the outer-reservoir parameter used in the trilinear-flow model is:

$$\beta_o = \sqrt{s/\eta_{OD}} \tanh\left[\sqrt{s/\eta_{OD}}(x_{eD} - 1)\right] \quad (3)$$

And the outer-reservoir parameter, α_o, used in trilinear- flow model is,

$$\alpha_o = \frac{\beta_o}{C_{RD} y_{eD}} + u \quad (4)$$

Hydraulic-fracture solution

The hydraulic fracture parameters used in the trilinear- flow model are:

$$\beta_F = \sqrt{\alpha_o} \tanh\left[\sqrt{\alpha_o}\left(y_{eD} - \frac{w_D}{2}\right)\right] \quad (5)$$

$$\alpha_F = \frac{2\beta_F}{C_{FD}} + \frac{s}{\eta_{FD}} \quad (6)$$

The dimensionless pressure solution for the hydraulic fracture is obtained as:

$$\bar{P}_{FD} = \frac{\pi}{C_{FD} s \sqrt{\alpha_F}} \frac{\cosh\left[\sqrt{\alpha_F}(1 - x_D)\right]}{\sinh(\sqrt{\alpha_F})} \quad (7)$$

Wellbore-pressure solution

The dimensionless wellbore pressure is obtained at $x_D = 0$ is given by,

$$\bar{P}_{wD} = \bar{P}_{FD}(x_D = 0) = \frac{\pi}{C_{FD} s \sqrt{\alpha_F} \tanh(\sqrt{\alpha_F})} \quad (8)$$

The skin factor caused by flow choking within the fracture is provided by Mukherjee and Economides (1991):

$$s_c = \frac{k_I h_I}{k_F w_F}\left[\ln\left(\frac{h}{2r_w}\right) - \frac{\pi}{2}\right] \quad (9)$$

The dimensionless wellbore pressure after the end of the radial flow in the hydraulic fracture:

$$\bar{P}_D = \frac{\pi}{C_{FD} s \sqrt{\alpha_F} \tanh(\sqrt{\alpha_F})} + \frac{s_c}{s} \quad (10)$$

The effect of wellbore storage was incorporated into the solution by substituting P_D from Equation (10) into the following convolution expression in the Laplace domain:

$$\bar{P}_{wD,storage} = \frac{\bar{P}_{wD}}{1 + C_D s^2 \bar{P}_{wD}} \quad (11)$$

The dimensionless wellbore storage coefficient, C_D, is given:

$$C_D = \frac{5.615C}{2\pi(\phi c h_t)_I x_F^2} \quad (12)$$

Dual-porosity parameters

The naturally-fractured reservoir parameters introduced by Warren and Root (1963) were used by Brown *et al*. (2011),

$$\omega = \frac{(\tilde{\phi}\tilde{c}_t)_f}{(\tilde{\phi}\tilde{c}_t)_f + (\tilde{\phi}\tilde{c}_t)_m} \quad (13)$$

$$\lambda = \sigma l^2 \frac{\tilde{k}_m}{\tilde{k}_f} \quad (14)$$

Where l is a reference length chosen as the half length of the hydraulic fracture; that is, $l = x_f$.

Kazemi *et al*. (1976) proposed the following first approximation for the shape factor of rectangular matrix blocks:

$$\sigma = 4\left(\frac{1}{L_x^2} + \frac{1}{L_y^2} + \frac{1}{L_z^2}\right) \quad (15)$$

Serra *et al*. (1983) define the storativity and flowcapacity ratios for the transient dual-porosity model, respectively, by:

$$\omega = \frac{(\phi c_t)_m}{(\phi c_t)_f} \quad (16)$$

$$\lambda = 12\left(\frac{l^2}{h_m^2}\right)\left(\frac{k_m h_m}{k_f h_f}\right) \quad (17)$$

The dimensionless oil pressure and the pressure derivative, respectively, are:

$$P_D = \frac{k_I h\left(P_i - P_{wf}\right)}{141.2\ B_o q_f \mu_o} \quad (18)$$

$$t_D * P_D' = \frac{k_f h(t * \Delta P')}{141.2\ q_f B_o \mu_o} \quad (19)$$

The dimensionless gas pseudopressure and the dimensionless pseudopressure derivative, respectively, for the constant-production-rate solution are:

$$P_D = \frac{k_I h\left[m(P_i) - m(P_{wf})\right]}{1424\ T\ q_f} \tag{20}$$

$$t_D * m(P_D)' = \frac{k_I h[t * \Delta m(P)']}{1424\ q_f T} \tag{21}$$

The dimensionless time is defined by;

$$t_D = \frac{\eta_I}{x_f^2} t \tag{22}$$

The inner-reservoir diffusivity,

$$\eta_I = \frac{0.0002637 k_I}{(\phi c_t)_I \mu} \tag{23}$$

The hydraulic-fracture diffusivity,

$$\eta_f = \frac{0.0002637 k_f}{(\phi c_t)_f \mu} \tag{24}$$

The outer-reservoir diffusivity,

$$\eta_o = \frac{0.0002637 k_o}{(\phi c_t)_o \mu} \tag{25}$$

The dimensionless distances in the x and y direction are defined, respectively, by

$$x_D = \frac{x}{x_f} \tag{26}$$

$$y_D = \frac{y}{x_f} \tag{27}$$

The dimensionless distances to the reservoir boundaries are given by x_{eD} and y_{eD}.

According to Brown *et al.* (2011), the pressure-transient response of a horizontal well with n_F identical transverse hydraulic fractures can be modeled by considering one of the fractures producing from a rectangular reservoir section at a rate:

$$q_f = \frac{q}{n_f} \tag{28}$$

The fracture is located centrally in the closed rectangular drainage area

$$A_{,drainage_f} = 2x_e \times 2y_e \tag{29}$$

The half-fracture length, x_f, can be related to reservoir length, x_e, by:

$$x_e = 2x_f \tag{30}$$

The dimensionless fracture and reservoir conductivities, respectively:

$$c_{fD} = \frac{k_f w_f}{\tilde{k}_I x_f} \tag{31}$$

$$c_{RD} = \frac{\tilde{k}_I x_f}{k_o y_e} \tag{32}$$

For any dual-porosity model, C_{FD} and C_{RD} are defined on the basis of the bulk permeability of the inner reservoir $\tilde{k}_I$. Brown *et al.* (2011) also defined the hydraulic fracture diffusivity and the outer-reservoir diffusivity ratios, respectively, as:

$$\eta_{fD} = \frac{\eta_f}{\eta_I} \tag{33}$$

$$\eta_{OD} = \frac{\eta_O}{\eta_I} \tag{34}$$

For the transient dual-porosity model:

$$k_I = k_f \tag{35}$$

$$h_I = n_f h_f \tag{36}$$

And the intrinsic fracture storativity is;

$$(\phi c_t)_I = (\phi c_t)_f \tag{37}$$

For the pseudosteady dual-porosity model:

$$k_I = \tilde{k}_f \tag{38}$$

$$h_I = h \tag{39}$$

And the intrinsic fracture storativity

$$(\phi c_t)_I = (\tilde{\phi}\tilde{c}_t)_f + (\tilde{\phi}\tilde{c}_t)_m \tag{40}$$

2.2. *TDS* formulation for pseudostady dual-porosity model

The Equations will be developed for oil flow. For gas flow refer to Appendix A and B. Even though, Brown *et. al.* (2011) presented pressure solutions for each flow regime, new simpler expressions based on the observations of the pressure derivative are derived in this work. However, a metholodology with the equations proposed by Brown *et. al.* (2011) for each flow regime is provided in Appendixes C and D.

2.2.1. Initial flow regime

The flow at early times displays a pressure derivative which slope goes from 0.25 to 0.5 depending upon the value of the storativity ratio, ω, as defined by Equation 13. This flow regime shows up at diferent times depending on the ω values, as shown in Figure-1. The early time portion of the log-log plot of the dimensionless pressure derivative versus dimensionless time curve under constant flow capacity ratio, λ, and variable storativity ratio, ω, is used for the determination of the initial flow regime governing equations.

For this model the developed equations depend on the storativity ratio value, ω. The estimated permeability value correponds to the one in the inner zone of the stimulated reservoir volume, SRV. To obtain an appropriate flow overning equation is necessary to adjust the application range according to the values the storativity ratio, ω.

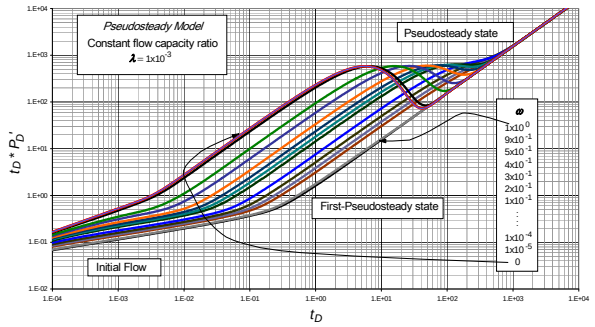

Figure-1. Effect of storativity ratio, ω, on the initial flow (early time) for the dual-porosity pseudosteady model under constant flow capacity ratio, λ, and y_D=x_D=1.

The determination of the governing equation for for $\omega \geq 0.1$ at early time requires a log-log plot of t_D*P_D' or t_D*$m(P)_D$' versus $t_D/(1+\omega)^4$ using a constant flow capacity ratio, λ, as shown in Figure-2. The initial flow is characterized by a typical 0.25-slope line (bilinear flow regime) on the pressure derivative curve.

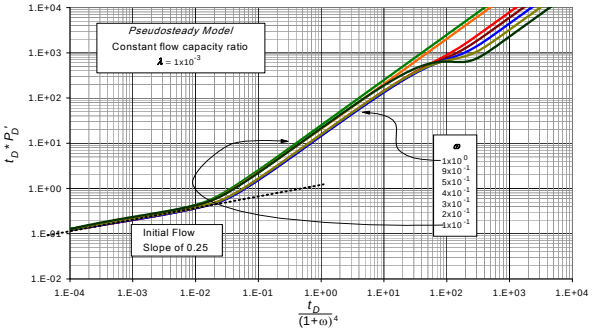

Figure-2. Effect storativity ratio, ω, on the initial flow for the case $\omega \geq 0.1$ on the pressure derivative behavior using the the dual-porosity pseudosteady model with constant flow capacity ratio, λ, and y_D=x_D=1

$$t_D * P_D' = 0.4159\pi \left(\frac{t_D}{(1+\omega)^4} \right)^{0.25} \tag{41}$$

Once the dimensionless quantities given by Equations (19), (22) and (23) are replaced into Equation (41), it yields;

$$\frac{k_I h[t * \Delta P']}{141.2\ q_f B_o \mu_o} = \frac{0.4159\pi}{(1+\omega)} \left(\frac{0.0002637 k_I t}{(\phi c_t)_I\ \mu x_f^2} \right)^{0.25} \tag{42}$$

Equation (42) allows solving for the permeability of the inner reservoir;

$$k_I = \left[\frac{24.9496\ q_f B_o \mu_o}{(1+\omega) h (t * \Delta P')} \left(\frac{t}{(\phi c_t)_I\ \mu x_f^2} \right)^{0.25} \right]^{\frac{1}{0.75}} \tag{43}$$

Notice that the hydraulic half- fracture length, x_f, can be solved from Equation (43),

$$x_f = \left[\frac{24.9496\ q_f B_o \mu_o}{(1+\omega) k_I^{0.75} h (t * \Delta P')_{BL}} \left(\frac{t_{BL}}{(\phi c_t)_I\ \mu} \right)^{0.25} \right]^2 \tag{44}$$

When $0.01 \leq \omega < 0.1$, the early flow is defined by a slope of 0.33 in a log plot of the pressure derivate. It gives a relationship of three log cycles in the time axis against two log cycles in the pressure derivative axis. As shown in Figure-3, the flow behavior does not present a uniformity related to the variation of ω, then, it was necessary to determine the most representative mathematical representation of the initial flow behavior which was performed by using a probabilistic average,

$$t_D * P_D' = 0.87847\pi\ t_D^{0.33} \tag{45}$$

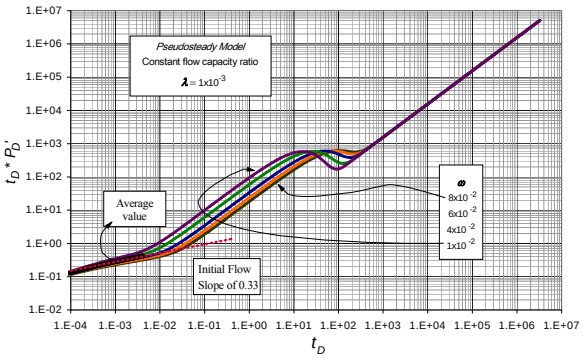

Figure-3. Initial flow behavior for the case $0.01 \leq \omega < 0.1$ on the pressure derivative behavior governed by the dual-porosity pseudosteady model with constant flow capacity ratio, λ, and y_D=x_D=1.

Once the dimensionless quantities given by Equations (19), (22) and (23) are replaced into Equation 45, it results;

$$\frac{k_I h(t*\Delta P')}{141.2\ q_f B_o \mu_o} = 0.87847\pi \left(\frac{0.0002637 k_I t}{(\phi c_t)_I \mu x_f^2} \right)^{0.33} \tag{46}$$

Equation (46) allows solving for the inner-reservoir permeability;

$$k_I = \left[\frac{25.685\, q_f B_o \mu_o}{h(t*\Delta P')_{TL}} \left(\frac{t_{TL}}{(\phi c_t)_I \mu x_f^2} \right)^{0.33} \right]^{\frac{1}{0.67}} \tag{47}$$

Notice that the half-fracture length, x_f, can be obtained from Equation (47),

$$x_f = \left[\frac{25.685\, q_f B_o \mu_o}{k_I^{0.67} h(t*\Delta P')_{TL}} \left(\frac{t_{TL}}{(\phi c_t)_I \mu} \right)^{0.33} \right]^{\frac{1}{0.66}} \tag{48}$$

Finally, the last case of ω variation at early time takes places for $0 < \omega < 0.01$ which is characterized by a half-slope (linear flow regime) in the pressure derivative log-log plot. A typical representation of the homogeneus reservoir occurs when ω=0 as depicted in Figure-4.

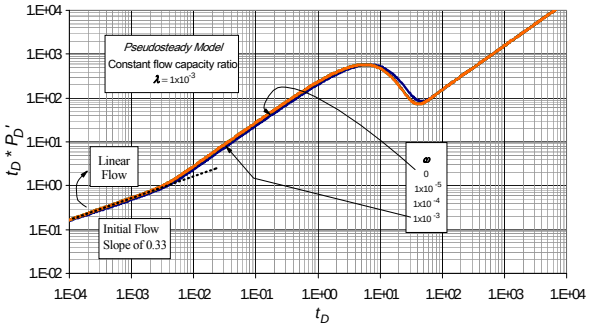

Figure-4. Initial flow pressure derivative behavior for $\omega < 0.01$ with dual-porosity pseudosteady model under constant flow capacity ratio, λ, and y_D=x_D=1.

$$t_D * (P_D)' = 5.35\pi \sqrt{t_D} \tag{49}$$

After plugging the dimensionless quantities into Equation (49), we obtain;

$$\frac{k_I h\left[t*(\Delta P)'\right]}{141.2\ q_f B_o \mu_o} = 5.35\pi \left(\frac{0.0002637 k_I t}{(\phi c_t)_I \mu x_f^2} \right)^{0.5} \tag{50}$$

Equation (50) allows solving for the permeability of the inner reservoir;

$$k_I = \left[\frac{38.5384\, q_f B_o \mu_o}{h(t*\Delta P')_L x_f} \left(\frac{t_L}{(\phi c_t)_I \mu} \right)^{0.5} \right]^2 \tag{51}$$

Notice that the half-fracture length, x_f, can also be solved from Equation (51),

$$x_f = \left[\frac{38.5384 q_f B_o \mu_o}{h(t*\Delta P')_L} \left(\frac{t_L}{(\phi c_t)_I \mu k_I} \right)^{0.5} \right] \tag{52}$$

For the three early-time cases the reservoir lenght can be solved from Equation (30) which depends only on the half- fracture length, x_f.

2.2.2. Second flow regime on first pseudosteady state

Once the initial flow regime vanishes, a second unit-slope flow regime is observed on the prssure derivative log-log plot. It has been arbitriarily refered here as "*first pseudosteady-state regime*" which is affected by both the flow capacity, λ, and the storativity ratios, ω. The former affects the duration time when the regime is presented as shown in Figure-5; thereby, the starting time of the first pseudosteady state regime converges at the same point for different λ values. With this parameter the flow regime varies in length but it is the same in terms of location (no parallel displacement along the time axis). In contrast, the storativity ratio, ω, causes a parallel displacement along the time axis as shown in Figure-6.

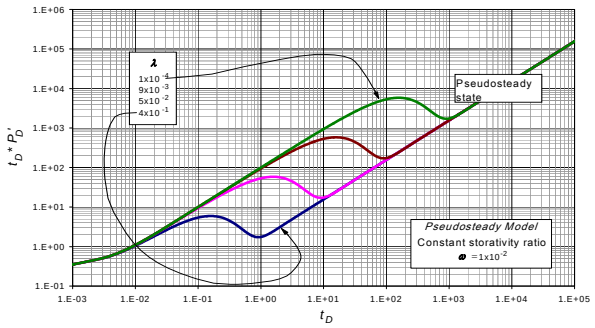

Figure-5. First pseudosteady state behavior observed in the dual-porosity pseudosteady model under constant storativity ratio, ω, and y_D=x_D=1.

The general equation for the unit-slope pseudosteady-state period is:

$$t_D*(P_D)' = b\ t_D \tag{53}$$

As the displacement along the time axis is defined by the value of storativity ratio, ω, it is possible to develop an expression to obtain b as a function of ω. These observations lead to obtain the following expression:

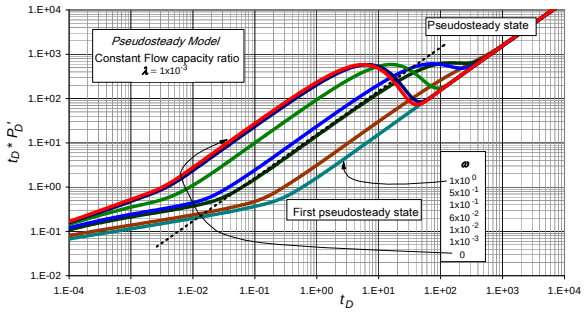

Figure-6. First pseudosteady state behavior observed in the dual-porosity pseudosteady model under constant flow capacity ratio, λ, and y_D=x_D=1.

1) Equation (54) which constants are given in Table-1 was developed to estimate b using the storativity ratio, ω. Its range of application is for values of $0 \le \omega < 1$.

$$b = \left[A + B\,\omega + C\,(\omega^{0.5}) \right]^{-1} \tag{54}$$

Table-1. Constants for Equation 54.

Constant	Value
A	0.00361707
B	0.646008952
C	-0.00058982

The b value obtained from Equation (54) is replaced into equation (53). It is important to point out that when ω=1, the first pseudosteady-state regime does not exist; then, the late-time pseudosteady-state period is only seen inidicating a homogeneous behavior. The storativity ratio, ω, only depends on fracture storativity. This represents the other extreme case where there is no matrix contribution.

Once the dimensionless quantities given by Equations (19), (22) and (23) are replaced into Equation (53), it yields;

$$\frac{k_I h\left[t*(\Delta P)'\right]}{141.2\ q_f B_o \mu_o} = b\left(\frac{0.0002637 k_I t}{(\phi c_t)_I\, \mu x_f^2}\right) \tag{54}$$

The first pseudosteady-state regime can be used to estimate either the hydraulic half-fracture length, x_f, or the well drainage area whether or not the permeability value is known.

$$x_f = \left[\frac{b\ 0.03723444\ q_f\ B_o}{h(\phi c_t)_I}\left(\frac{t_{qPSS}}{\left[t*\Delta P'\right]_{qPSS}}\right)\right]^{\frac{1}{2}} \tag{55}$$

Finally, drainage area and half-reservoir length, x_e, can be computed using equations (29) and (30), respectively.

2.2.3. Late-time pseudosteady-state regime

Pseudosteady-state is the last flow regime that can be seen in a test run long enough in the systems we are dealing with. This is recognized by a unit-slope straight line. It is important to remark that in transient-pressure analysis for the dual-porosity pseudosteady model, this behavior is independent of the flow capacity ratio, λ, and the storativity ratio, ω; see Figures-5 and 6; however, the behavior of the late pseudosteady-state regime is particular for different dimensionless length values (y_D= 0.35, 0.5, 075 and 1), as shown in Figure-6.

For this reason the determination of the governing equation for the late pseudosteady period requires a log-log plot of t_D*P_D' or $t_D*m(P)_D$' versus t_{DA} using a constant parameter of flow-capacity ratio and storativity ratio (λ and ω = constant) and different dimensionless length values (y_D= 0.35, 0.5, 075 and 1), as shown in Figure-7. In each case, a uniform behavior was found by dividing the dimensionless time by the dimensionless length of the stimulated reservoir volume for each case, respectively.

$$t_{DA} = \frac{t_D}{y_D^2} \tag{56}$$

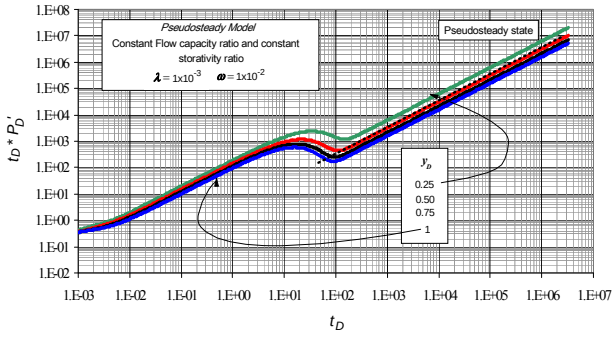

Figure-7. Effect of the variation of the dimensionless length on the pseudosteady-state period for the late pseudosteady-state period in the dual-porosity pseudosteady model with constant flow capacity ratio, λ, and constant storativity ratio, ω.

Then, it is possible to write a general dimensionless pressure or pseudopressure derivative expression for the pseudosteady-state period, as follows,

$$\frac{[t_D * P_D']_{PSS}}{y_D} = 0.4973\pi \left(\frac{t_D}{y_D^2} \right)_{PSS} \quad (57)$$

Once the dimensionless terms given by Equations (19), (22) and (23) are replaced in Equation (57), an expression for the determination of the half- fracture length, x_f, is obtained,

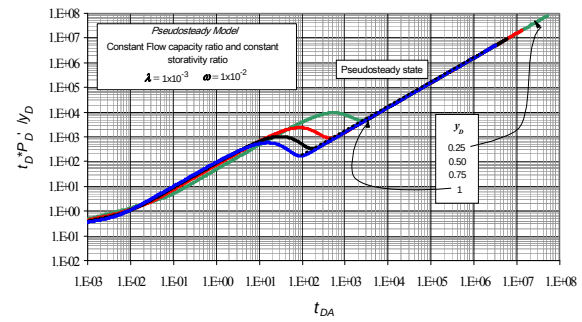

Figure-8. Effect of the variation of the dimensionless length on the late pseudosteady-state period for the dual-porosity pseudosteady model with constant flow capacity ratio, λ and constant storativity ratio, ω.

$$x_f = \frac{0.058172\, B_o q_f}{h_f (\phi c_t)_f\, y} \frac{t_{PSS}}{[t * \Delta(P)']_{PSS}} \quad (58)$$

Notice that x_f can be solved from Equations (55) and (58) whether or not the permeability value is known. For this reason is possible calculate the distance y-coordinate.

$$y = \frac{0.058172\, B_o q_f}{h_f (\phi c_t)_f\, x_f} \frac{t_{PSS}}{[t * \Delta(P)']_{PSS}} \quad (59)$$

2.2.4. Dimensionless storativity, ω, ratio and flow capacity ratio, λ

The calculation of the flow capacity ratio, λ, and storativity ratio, ω, use the transition period observed in a log-log plot of the dimensionless pressure derivative versus dimensionless time which is characterized by a trough and permits defining correlations to estimate the above-mentioned parameters.

The maximum peak found on the pressure derivative was correlated to calculate, λ, this characteristic points were chosen since it is independent of ω as pointed out in Figure-9.

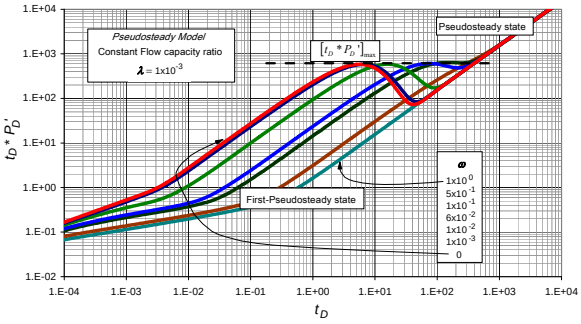

Figure-9. Effect of storativity ratio, ω, on the maximum point (peak) pressure derivative during the start of the transition period for the dual-porosity pseudosteady model.

Using the dimensionless pressure derivative value at the peak during the start of transition period $(t_D * P_D')_{max}$ allows obtaining:

$$\lambda = \left[A + B[t_D * P_D']_{max} + \frac{C}{[t_D * P_D']_{max}} \right]^{-1} \quad (60)$$

The range of application of Equation (60) is for $1x10^{-5} \leq \lambda < 1$. That applies to extreme cases. Constants A through C are given in Table-2.

Table-2. Constants for Equation (60).

Constant	Value
A	-0.22892364
B	1.693500511
C	0.004208008

The minimum point (trough) of the pressure derivative, $(t_D * P_D')_{min}$, is used to evaluate the storativity ratio, ω. This point, however, is affected by λ, then, a correct equation for ω computation should include, so that:

$$\omega = A + B[(t_D * P_D')_{min} * \lambda] + C[(t_D * P_D')_{min} * \lambda]^3 \quad (61)$$

Constants *A* through *C* are given in Table-3.

Table-3. Constants for Equation (61).

Constant	Value
A	-0.00674835
B	0.090506793
C	0.205670929

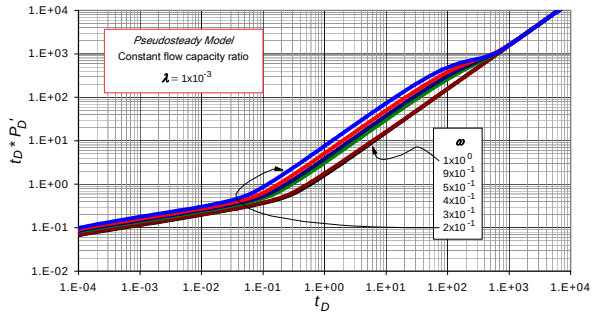

Figura-10. Absence of the trough when $\omega > 0.1$ in the dual- porosity pseudosteady model, λ constant and $y_D=x_D$.

The range of application of Equation (61) is $1x10^{-3} \leq \omega \leq 0.1$. This range applies when the transition period is evident in the pressure derivative vs. time log-log because for ω values greater than 0.1, see Figure-10, the minimum point (trough) is not seen which prevents finding a characteristic point to develop an expression in these cases. It is important to clarify that the above developed equations were obtained considering $y_D=x_D=1$.

2.3. *TDS* formulation for transient dual-porosity model

2.3.1 Initial flow regime

This is presented for all values of the flow capacity ratio, λ, and the storativity ratio, ω defined by Equations (16) and (17), respectively, during the bilinear flow regime on the pressure derivative curve as shown in Figures (10) and (11). This means that the initial flow is independent of the λ and ω values.

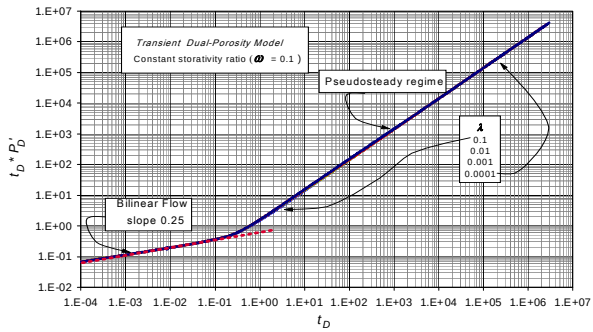

Figure-11. Effect of the flow capacity ratio, λ, on the bilinear flow regime for the transient dual-porosity model, with $\omega = 0.1$.

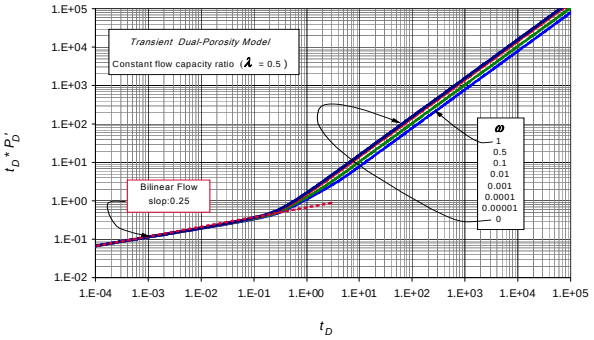

Figure-12. Effect of the storativity ratio, ω, on the bilinear flow regiem for transient dual-porosity model, with $\lambda = 0.5$.

The bilinear flow regime also takes place at about the same period of time for the different y_D values as shown in Figure-13. Therefore, its behavior does not depend upon neither the variation of the dimensionless reservoir length, y_e, nor the λ and ω parameters.

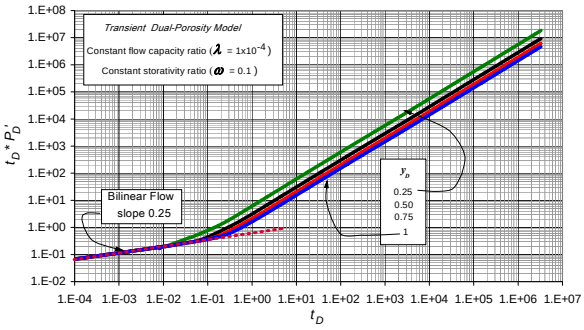

Figure-13. Effect of the dimensionless reservoir length, y_D, variation on the bilinear flow regime for the transient dual-porosity model, with constant values of λ and ω.

Then, at early time the flow is governed by the following equation:

$$\left[t_D * P_D{}'\right] = 0.2052\,\pi\sqrt{t_D} \tag{61}$$

Once the dimensionless quantities given by Equations (19), (22) and (23) are replaced into Equation 61, it yields;

$$\frac{k_I h\left[t*(\Delta P)'\right]}{141.2\ q_f B_o \mu_o} = 0.2052\,\pi\left(\frac{0.0002637 k_I t}{(\phi c_t)_I\,\mu x_f^2}\right)^{0.25} \tag{62}$$

Equation (62) allows solving for the inner-reservoir permeability as follows;

$$k_I = \left[\frac{11.60\,q_f B_o \mu_o}{h_I (t*\Delta P')_{BL}}\left(\frac{t_{BL}}{(\phi c_t)_I\,\mu x_f^2}\right)^{0.25}\right]^{\frac{1}{0.75}} \tag{63}$$

Notice that the hydraulic half-fracture length, x_f, can also be solved from Equation (63),

$$x_f = \left[\frac{11.60\, q_f B_o \mu_o}{k_I^{0.75} h (t*\Delta P')_{BL}} \left(\frac{t_{BL}}{(\phi c_t)_I \, \mu} \right)^{0.25} \right]^2 \qquad (64)$$

2.3.2. Pseudosteady-state period

This is recognized by a unit-slope straight line on the pressure derivative curve. It is important to note that, contrary to the dual-porosity pseudosteady-state model, the transient model has only one pseudosteady-state period since this models assumes that $k_I = k_f$, therefore, the first pseudosteady-sate period is absent. Additionally, for this model, the pressure transient behavior is not fully independent of both the flow capacity ratio, λ, and storativity ratio, ω, since there exists a restricction in the uniformity ranges of the model showing a variation of the intersection point, b, as a function of ω for λ values greater than 0.5 or for the contrary case where the intersection point, b, is a function of λ for ω values greater than 0.5 as observed in Figure-14. In other words, the developed equation for pseudosteady state in restricted to ω and $\lambda >$ 0.5. However, the uniformity is kept for the remaining values of flow-capacity-, λ, and storativity-, ω, values. This becomes more evident at the beginning of the pseudosteady-state period as shown in Figures-15 and 16.

The behavior of the late pseudosteady-state period is particular for different dimensionless reservoir length values (y_D = 0.35, 0.5, 075 and 1), as shown in Figures-17.

As for the pseudosteady-state model, the determination of the governing equation for the late pseudosteady period requires a log-log plot of t_D*P_D' or $t_D*(mP)_{D'}$ versus t_{DA} using a constant parameter of flow capacity ratio and storativity ratio (λ and ω constant) and different dimensionless reservoir length values (y_D= 0.35, 0.5, 075 and 1), as shown in Figure-18.

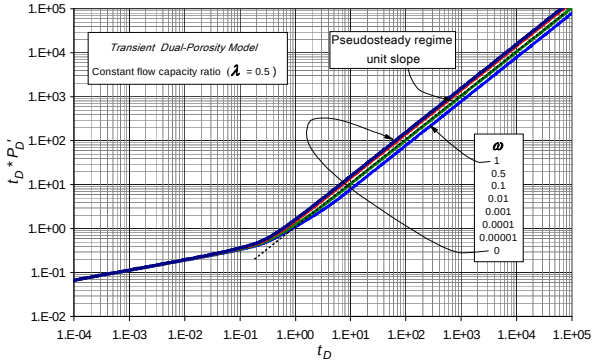

Figure-14. Effect of the storativity ratio, ω, on the pseudosteady-state regime for the transient dual-porosity model, with constant flow capacity ratio, λ = 0.5.

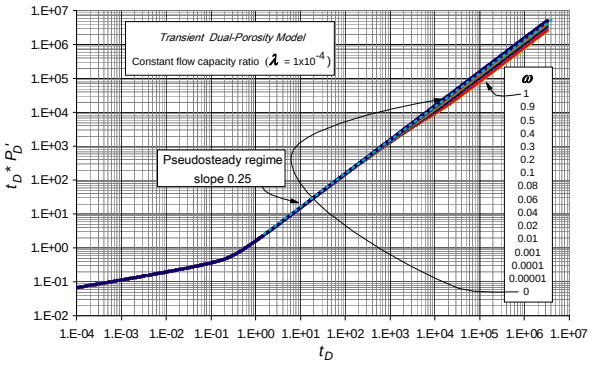

Figure-15. Effect of the storativity ratio, ω, on the pseudosteady-state period for the transient dual-porosity model, with constant flow capacity ratio ($\lambda = 1x10^{-4}$).

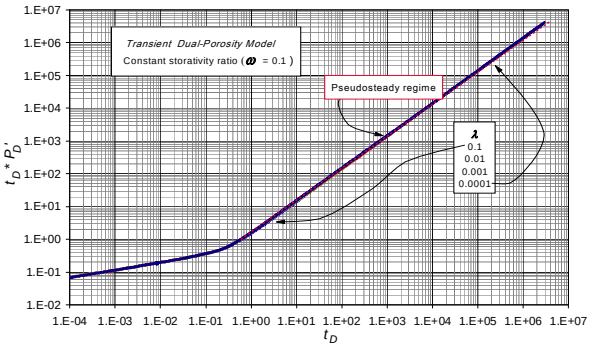

Figure-16. Effect of the flow capacity ratio, λ, on the bilinear flow regime for the transient dual-porosity model, with constant storativity ratio (ω = 0.1).

In each case, a uniform behavior was found by dividing the dimensionless time by the dimensionless length of the stimulated reservoir volume for each particular case, respectively.

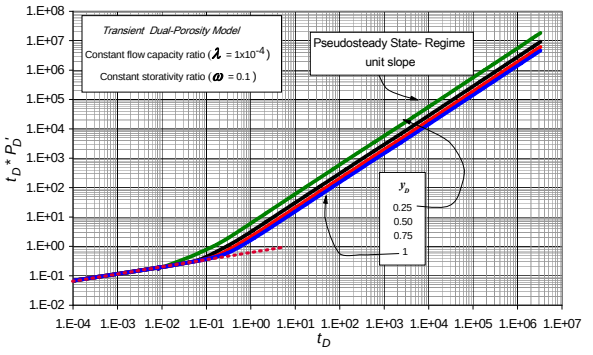

Figure-17. Effect of the dimensionless reservoir length variation, y_D, on the bilinear flow regime for the transient dual-porosity model, with constant λ and ω.

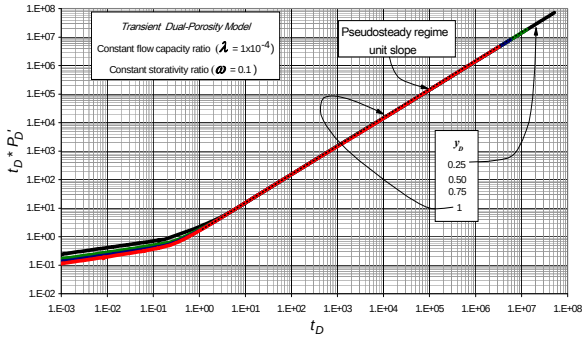

Figure-18. Effect of the dimensionless reservoir length variation on the pseudosteady-state regime for the pseudosteady-state period for the dual-porosity transient model, with constant flow capacity ratio, λ, and constant storativity ratio, ω.

$$t_{DA} = \frac{t_D}{y_D^2} \tag{65}$$

Then, it is possible to write a general dimensionless pressure or pseudopressure derivative expression for the pseudosteady-state period, as follows,

$$\frac{[t_D * P_D']_{PSS}}{y_D} = 0.4933\pi \left(\frac{t_D}{y_D^2} \right)_{PSS} \tag{66}$$

After the dimensionless terms given by Equations (19), (22), (23) and (65) are replaced in Equation 66, an expression for the determination of the half- fracture length, x_f, is obtained,

$$x_f = \frac{0.05770\, B_o\, q_f}{h_I (\phi c_t)_I\, y} \frac{t_{PSS}}{[t * \Delta(P)']_{PSS}} \tag{67}$$

Notice that the hydraulic-fracture half-length, x_f, can be solved from Equation (59), since Equation (67) makes possible the calculation of the distance y-coordinate.

$$y = \frac{0.05770\, \beta\, q_f}{h_I (\phi c_t)_I\, x_f} \frac{t_{PSS}}{[t * \Delta(P)']_{PSS}} \tag{68}$$

4. EXAMPLES

Two synthetic examples are worked out for the applicability of the above developed equations, one for each model. Table-4 provides relevant information of the reservoir, well and fluid properties used for the dual-porosity pseudosteady-state model.

Table-4. Relevant information for example of the dual-porosity pseudosteady model.

Parameter	Value	Parameter	Value
h (ft)	200	k_f, md	$1x10^4$
r_w (ft)	0.3	k_I, md	$1x10^{-2}$
μ_O (cp)	2.2	k_o, md	$2.0x10^{-3}$
β_O (bbl/STB)	1.08	q_f (bbl/day)	2500
Ω	0.0052	λ	0.0083
x (ft)	1325	y (ft)	1325
φ_f	0.45	c_{tf} (1/psi)	$3x10^{-1}$
φ_I	0.12	c_{tI} (1/psi)	$1x10^{-4}$
φ_O	0.1	c_{tO} (1/psi)	$3x10^{-4}$
x_f (ft)	1325	w_f (ft)	0.01
η_{fD}	88.9	η_{oD}	$8\ x10^{-2}$

For the case under consideration the pressure drop and its derivative against time are reported in Figures-19 and 20 with the purpose of determining the inner reservoir permeability or the half-fracture length depending upon the model type, half-fracture length and reservoir length, which will be obtained by using the equations developed in this work. The other permeability values could be estimated using the expressions provided by Brown *et al.* (2011) according to the diffusivity ratio. The computations will be outlined as follows.

4.1. Example-1. Pseudosteady model

Considerations given by Equations 35 through 37 should be taken into account in this model. The information provided in Table-4 and Figure-19 is useful for the estimation of the inner reservoir permeability, k_I, the reservoir length and half-fracture length.

Solution. As expected for this example, linear flow is observed at early times followed by the first pseudosteady-state period taking place before the transition period (trough). Finally, the late pseudosteady-state period is observed. The following information was read from Figure-19.

$t_L = 2636.4334$ hr
$[t*\Delta P']_L = 7.5305x10^4$ psi
$t_{qPSS} = 8.4981x10^5$ hr
$[t*\Delta P']_{qPSS} = 2.8389x10^6$ psi
$t_{PSS} = 1.7508x10^9$ hr
$[t*\Delta P']_{PSS} = 6.5267x10^7$ psi

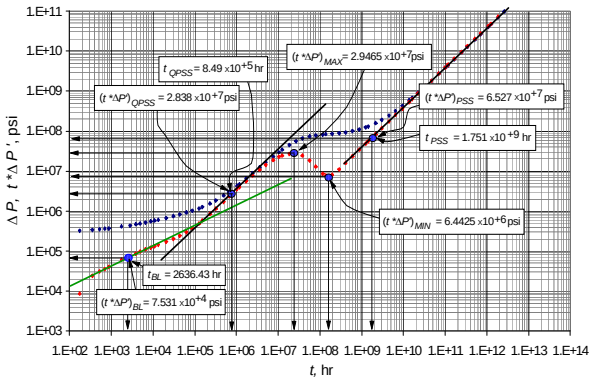

Figure-19. Log-log plot of the pressure and pressure derivative vs. time for the dual-porosity pseudosteady model synthetic example.

It is also required to read the parameters during the transition period which are useful for estimating ω and λ.

$[t*\Delta P']_{max} = 2.9465 \times 10^7$ psi
$[t*\Delta P']_{min} = 6.4425 \times 10^6$ psi

It is recommended to use the unit-slope pseudosteady state periods to estimate x_f without needing the inner reservoir permeability value which is carried out by using Equation (58) to provide x_f = 1324.97 ft. An x_e value of 2649.94 ft is found with Equation (30). Now, by taking a glance to Equation (55), which applies on the late time pseudosteady-state period, requires the value of b, which resulted to be 144.22 by using Equation (54). Applying this value into Equation (55) gives an x_f value of 1344.76 ft and x_e 2689.54 ft. The last value is the one recommended for the reservoir area/length.

The estimation of k_I uses the initial time period which is dominated by linear flow regime (half slope). Then, the use of Equation (47) provides a value of 0.013 md and Equation (48) gives an x_f value of 1332.18 ft.

Finally, application of Equations (60) and (61) allows for the estimation of the λ and ω naturally-fractured parameters. For such purpose the peak and trough pressure derivative values have to be converted to dimensionless form. This is performed by using Equation (19) which provides 70.260(max) and 15.363(trough), respectively. Then, Equations 60 and 61 allow obtaining values of 0.0084 and 0.0054 for λ and ω, respectively.

4.2. Example-2. Transient model

It is required to find permeability, reservoir length and half-fracture length from the data reported in Figure-20 and the information given in Table-5.

Solution. As expected for this example, only two flow regimes are observed. First, linear flow regime which is followed by late pseudosteady-state period. The naturally-fractured typical transition period is absent. The below parameters were read from Figure-20;

Table-5. Relevant information for the transient model of dual- porosity.

Parameter	Value	Parameter	Value
h (ft)	200	k_f, md	$1x10^4$
r_w (ft)	0.3	k_I, md	$1x10^{-2}$
μ_O (cp)	2.2	k_o, md	$2.0x10^{-3}$
B_O (bbl/STB)	1.08	q_f (bbl/day)	2500
Ω	0.0052	λ	0.0083
x (ft)	725	y (ft)	350
ϕ_f	0.45	c_{tf} (1/psi)	$3x10^{-1}$
ϕ_I	0.12	c_{tI} (1/psi)	$1x10^{-4}$
ϕ_O	0.1	c_{tO} (1/psi)	$3x10^{-4}$
x_f (ft)	725	w_f (ft)	0.01
η_{fD}	88.9	η_{oD}	$8 x10^{-2}$

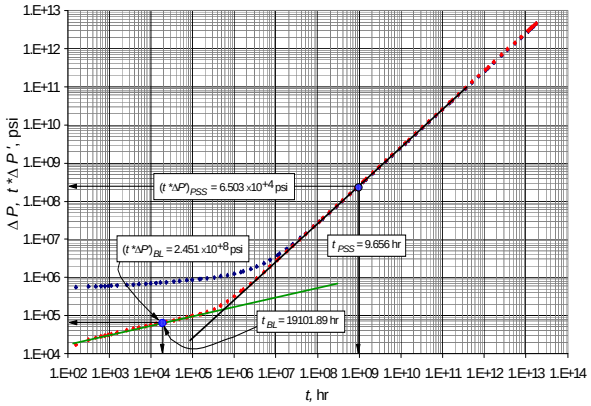

Figure-20. Log-log plot of the pressure and pressure derivative vs. time for transient dual-porosity model synthetic example.

$t_L = 2636.4334$ hr
$[t*\Delta (P)']_{BL} = 7.5305 \times 10^4$ psi
$t_{PSS} = 1.7508 \times 10^9$ hr
$[t*\Delta(P)']_{PSS} = 6.5267 \times 10^7$ psi

It is recommended as a methodic procedure to use Equation (63) which applies on the late pseudosteady-state period to obtain an x_f value de 730.6 ft. A value of x_e equal to 1461.2 ft is found with Equation (30). Also, the pseudosteady-state period is used to estimate the reservoir distance in the y direction, Equation (68), which resulted to be 352.7 ft.

Now, Equation (63) is used to find a k_I value of 0.0103 md and an x_f of 754.98 ft is estimated with Equation 64.

5. CONCLUSIONS

a) New expressions for the interpretation of pressure-transient tests in shale formations using both transient

and pseudosteady-state models are obtained by using characteristic points found on the pressure and pressure derivative versus time log-log plot. The equations were successfully tested with simulated examples so half-fracture length, inner-reservoir permeability and reservoir dimensions were found with a very good agreement with the input data. This study did not consider the variations of the diffusivity parameters η_{fD} and η_{oD}.

b) Contrary to the transient model, the pseudosteady state dual-porosity model displays the transition period (trough) characteristic of naturally-fractured formations. Besides, this model displays a unit-slope pseudosteady-state period called here as "First pseudosteady state". The transient model has no transition period and the influence of λ and ω is evident when this parameters are greater than 0.5. Then, it is recommended to analyze the behavior of the ranges of λ and ω to find expressions to allow their estimations.

c) The models were used assuming square reservoir geometry. However, the expressions for the late pseudosteady-state period were corrected for rectangular geometries.

ACKNOWLEDGEMENTS

The authors gratefully thank the Most Holy Trinity and the Virgin Mary mother of God for all the blessing received during their lives.

REFERENCES

Bernal K.M., Escobar F.H. and Ghisays-Ruiz A. 2014. Pressure and Pressure Derivative Analysis for Hydraulically-Fractured Shale Formations Using the Concept of Induced Permeability Field. Journal of Engineering and Applied Sciences. ISSN 1819-6608. 9(9). Accepted for publication.

Brown M., Ozkan E., Raghavan R. and Kazemi H. 2011. Practical Solutions for Pressure-Transient Responses of Fractured Horizontal Wells in Unconventional Shale Reservoirs. SPE Reservoir Evaluation and Engineering. pp. 663-676.

Cinco-Ley H. and Meng H.Z. 1988. Pressure Transient Analysis of Wells with Finite Conductivity Vertical Fractures in Double Porosity Reservoirs. Society of Petroleum Engineers. Doi: 10.2118/18172-MS.

Escobar F.H., Montenegro L.M. and Bernal K.M. 2014. Transient-Rate Analysis For Hydraulically-Fractured Gas Shale Wells Using The Concept Of Induced Permeability Field. Journal of Engineering and Applied Sciences. ISSN 1819-6608. 9(8): 1244-1254.

Chen C.-C. and Raghavan R. 1997. A Multiply-Fractured Horizontal Well in a Rectangular Drainage Region. SPE J. 2(4): 455-465. SPE-37072-PA.

El-Banbi A., H. and Wattenbarger R.A. 1998. Analysis of Linear Flow in Gas Well Production. Paper SPE 39972 presented at the SPE Gas Technology Symposium, Calgary, Alberta, Canada.

Ge J. and Ghassemi A. 2011. Permeability Enhancement in Shale Gas Reservoirs after Stimulation by Hydraulic Fracturing. Paper AR11-514 presented at the Rock Mechanics / Geomechanics Symposium, San Francisco, CA.

Kazemi H., Merrill L. S., Porterfield K. L. and Zeman P. R. 1976. Numerical Simulation of Water-Oil Flow in Naturally Fractured Reservoirs. Society of Petroleum Engineers. doi:10.2118/5719-PA.

Mukherjee H. and Economides M. J. 1991. A Parametric Comparison of Horizontal and Vertical Well Performance. Society of Petroleum Engineers. doi:10.2118/18303-PA.

Serra K., Reynolds A. C. and Raghavan R. 1983. New Pressure Transient Analysis Methods for Naturally Fractured Reservoirs(includes associated papers 12940 and 13014). Society of Petroleum Engineers. doi:10.2118/10780-PA.

Tiab D. 1993. Analysis of Pressure and Pressure Derivative without Type-Curve Matching: 1- Skin and Wellbore Storage. Journal of Petroleum Science and Engineering. 12: 171-181.

APPENDIX- A. GOVERNING EQUATIONS FOR GAS FLOW DUAL-POROSITY PSEUDOSTEADY MODEL

A.1. Initial flow

- $\omega \geq 0.1$

The initial flow is characterized by a typical 0.25-slope line on the pressure derivative curve, the behavior is given by:

$$t_D * (mP_D)' = 0.4159\pi \left(\frac{t_D}{(1+\omega)^4} \right)^{0.25} \quad (A.1)$$

Once the dimensionless terms given by Equations (19), (22) and (23) are plugged into Equation A.1 and solving for the inner reservoir permeability, it yields,

$$k_I = \left[\frac{237.097\, q_f T}{(1+\omega)h\left[t * \Delta(mP)'\right]} \left(\frac{t}{(\phi c_t)_I\, \mu x_f^2} \right)^{0.25} \right]^{\frac{1}{0.75}} \quad (A.2)$$

From the above equation it is possible to find the value of the hydraulic half- fracture length, x_f:

$$x_f = \left[\frac{237.097\, q_f T}{(1+\omega) k_I^{0.75} h\left[t * \Delta(mP)'\right]} \left(\frac{t}{(\phi c_t)_I\, \mu} \right)^{0.25} \right]^2 \quad \text{(A.3)}$$

- $\leq \omega < 0.1$

The initial flow characterized by a typical 0.33-slope line on the pressure derivative curve, the behavior is given by:

$$t_D * (mP_D)' = 0.87847\pi\ t_D^{0.33} \quad \text{(A.4)}$$

Once the dimensionless quantities expressed by Equations (19), (22) and (23) are replaced into Equation (A.4), the permeability of the inner reservoir; can be solved for:

$$k_I = \left[\frac{259.0318\, q_f T}{h\left[t * \Delta(mP)'\right]} \left(\frac{t}{(\phi c_t)_I\, \mu x_f^2} \right)^{0.33} \right]^{\frac{1}{0.67}} \quad \text{(A.5)}$$

From the above equation it is also possible to solve for the value of the half- fracture length, x_f:

$$x_f = \left[\frac{259.0318\, q_f T}{k_I^{0.67} h\left[t * \Delta(mP)'\right]} \left(\frac{t}{(\phi c_t)_I\, \mu} \right)^{0.33} \right]^{\frac{1}{0.66}} \quad \text{(A.6)}$$

- $0 < \omega < 0.01$

The initial flow is characterized by a typical 0.5-slope line on the pressure derivative curve which behavior is governed by:

$$t_D * (mP_D)' = 5.35\pi \sqrt{t_D} \quad \text{(A.7)}$$

Once the dimensionless terms given by Equations (34), (35) and (36) are plugged into Equation (A.7) and solving for the inner reservoir permeability;

$$k_I = \left[\frac{388.69\, q_f T}{h\left[t * \Delta(mP)'\right] x_f} \left(\frac{t}{(\phi c_t)_I\, \mu} \right)^{0.5} \right]^2 \quad \text{(A.8)}$$

Also, from the above equation the half-fracture length, x_f, can be solved for;

$$x_f = \left[\frac{388.66\, q_f T}{h\left[t * \Delta(mP)'\right]} \left(\frac{t}{(\phi c_t)_I\, \mu k_I} \right)^{0.5} \right] \quad \text{(A.9)}$$

A.2. Second flow regime or first pseudosteady state

The general equation for the pseudosteady state with unit-slope line is:

$$t_D * (mP_D)' = b\ t_D \quad \text{(A.10)}$$

Since the displacement along the time axis is a function of the storativity ratio, ω, is possible to develop an expression to obtain b as a function of it.

$$b = \left[A + B\,\omega + C\,(\omega^{0.5}) \right]^{-1} \quad \text{(A.11)}$$

Constants *A* through *C* are given in Table-6.

Table-6. Constants for Equation (A.11).

Constant	Value
A	0.00361707
B	0.646008952
C	-0.00058982

The range of application of Equation (A.11) goes for $0 \leq \omega < 1$. The first pseudosteady-state regime can be used for the computaion of, x_f,

$$x_f = \left[\frac{b\ 0.3755\ q_f\, T}{h(\phi c_t \mu)_I} \left(\frac{t}{\left[t * (\Delta P)'\right]} \right) \right]^{\frac{1}{2}} \quad \text{(A.12)}$$

A.3. Pseudosteady-state regime

Once the dimensionless terms given by Equations (19), (22), (23) and (65) are replaced in Equation (57), an expression for the determination of of the hydraulic half-fracture length, x_f, is obtained,

$$x_f = \frac{0.5867 T q_f}{h_I (\phi c_t \mu)_I\, y} \frac{t_{PSS}}{\left[t * \Delta(mP)'\right]_{PSS}} \quad \text{(A.13)}$$

A.4. Dimensionless storativity (ω) ratio and flow-capacity ratio (λ)

The calculation of the parameters flow-capacity ratio (λ) and storativity ratio (ω) is the same for goberning expressions for oil model.

APPENDIX- B. GOVERNING EQUATIONS FOR GAS FLOW TRANSIENT DUAL-POROSITY MODEL

B.1. Initial Flow

The initial flow characterized by a 0.25-slope line on the pressure derivative curve is governed by;

$$\left[t_D * P_D'\right] = 0.2052\,\pi \sqrt{t_D} \quad \text{(B.1)}$$

After replacing the dimensionless terms provided by Equations (19), (22) and (23) in Equation B.1 and solving for the of the inner reservoir permeability, we obtain:

$$k_I = \left[\frac{116.98\, q_f T}{h_I \left[t * \Delta(mP)'\right]} \left(\frac{t}{(\phi c_t)_I\, \mu x_f^2} \right)^{0.25} \right]^{\frac{1}{0.75}} \quad \text{(B.2)}$$

From the above equation it is possible to find the value of the hydraulic half- fracture length, x_f:

$$x_f = \left[\frac{116.98 q_f T}{k_I^{0.75} h \left[t * \Delta(mP)' \right]} \left(\frac{t}{(\phi c_t)_I \mu} \right)^{0.25} \right]^2 \quad \text{(B.3)}$$

B.2. Pseudosteady-state regime

After plugging the dimensionless terms given by Equations (19), (22), (23) and (65) in Equation (57), an expression for the determination of x_f is obtained,

$$x_f = \frac{0.5819 T q_f}{h_I (\phi c_t \mu)_I y} \frac{t_{PSS}}{\left[t * \Delta(mP)' \right]_{PSS}} \quad \text{(B.4)}$$

APPENDIX- C. GOVERNING EQUATIONS FOR ASYMPTOTIC SOLUTIONS FOR PRESSURE AND DERIVATIVE: PSEUDOSTEADY DUAL-POROSITY MODEL

C.1. Early time

The slope of straight line on log P_D vs. log t_D and log [t_D*P_D'] vs. log t_D is 1.

$$\left(t_D * P_{wD}' \right) = \frac{t_D}{C_D} \quad \text{(C.1)}$$

$$C = \frac{0.04167 q_f B_o h_t}{h_I} \frac{t}{(t * \Delta P')} \quad \text{(C.2)}$$

$$C = \frac{0.4202 q_{fg} T_t}{h_I} \frac{t}{\left[t * \Delta(mP') \right]} \quad \text{(C.3)}$$

For pressure;

$$P_D = \frac{t_D}{C_D} \quad \text{(C.4)}$$

$$C = \frac{0.04167 q_f B_o h_t}{h_I} \frac{t}{\Delta P} \quad \text{(C.5)}$$

$$C = \frac{0.4202 q_f T_t}{h_I} \frac{t}{\Delta m(P)} \quad \text{(C.6)}$$

C.2 Intermediate time

The slope of straight line on log P_D vs. log t_D and log [t_D*P_D'] vs. log t_D is 0 and -∞ respectibility.

$$\left(t_D * P_D' \right) = 0 \quad \text{(C.7)}$$

$$\left[t_D * m(P_D)' \right] = 0 \quad \text{(C.8)}$$

For pressure,

$$P_D = \frac{\pi(1-\omega)}{2 y_{eD} \lambda} + \frac{\pi y_{eD}}{6} + \frac{\pi}{3 C_{FD}} + s_c \quad \text{(C.9)}$$

If s_c=0

$$k_I = \frac{141.2 q_f \beta_o \mu}{h_I \Delta P} \left(\frac{\pi(1-\omega)}{2(y_e / y_F)\lambda} + \frac{\pi(y_e / y_F)}{6} + \frac{\pi}{3 \frac{k_F w_F}{k_I x_F}} \right) \quad \text{(C.10)}$$

$$k_I = \frac{1424 q_f T}{h_I (\Delta mP)} \left(\frac{\pi(1-\omega)}{2(y_e / y_F)\lambda} + \frac{\pi(y_e / y_F)}{6} + \frac{\pi}{3 \frac{k_F w_F}{k_I x_F}} \right) \quad \text{(C.11)}$$

The slope of straight line on log P_D vs. log t_D and log [t_D*P_D'] vs. log t_D is 0 and -∞ respectibility.

$$\left(t_D * P_D' \right) = 0 \quad \text{(C.12)}$$

$$\left[t_D * m(P_D)' \right] = 0 \quad \text{(C.13)}$$

For pressure,

$$P_D = \frac{\pi}{\sqrt{2 C_{FD}}} \left(\frac{1-\omega}{\lambda} \right)^{1/4} + s_c \quad \text{(C.14)}$$

If s_c=0

$$k_I = \frac{141.2 q_f \beta_o \mu}{h_I \Delta P} \left(\frac{\pi}{\sqrt{2 \frac{k_F w_F}{k_I x_F}}} \left(\frac{1-\omega}{\lambda} \right)^{1/4} \right) \quad \text{(C.15)}$$

$$k_I = \frac{1424 q_f T}{h_I \Delta m(P)} \left(\frac{\pi}{\sqrt{2 \frac{k_F w_F}{k_I x_F}}} \left(\frac{1-\omega}{\lambda} \right)^{1/4} \right) \quad \text{(C.16)}$$

The slope of straight line on log P_D vs. log t_D and log [t_D*P_D'] vs. log t_D is 0 and -∞ respectibility.

$$\left(t_D * P_D' \right) = 0 \quad \text{(C.17)}$$

$$\left[t_D * m(P_D)' \right] = 0 \quad \text{(C.18)}$$

For pressure,

$$P_{wD} = \frac{\pi}{2} \sqrt{\frac{1-\omega}{\lambda}} + \frac{\pi}{3 C_{FD}} + s_c \quad \text{(C.19)}$$

If s_c=0

$$k_I = \frac{221.796\, q_f B_o \mu_o}{h_I \Delta P}\left(\sqrt{\frac{1-\omega}{\lambda}} + \frac{\pi}{3\frac{k_F w_F}{\bar{k}_I x_F}}\right) \quad \text{(C.20)}$$

$$k_I = \frac{2236.814\, q_f T}{h_I \Delta m(P)}\left(\sqrt{\frac{1-\omega}{\lambda}} + \frac{\pi}{3\frac{k_F w_F}{\bar{k}_I x_F}}\right) \quad \text{(C.21)}$$

The slope of straight line on log P_D vs. log t_D and log [t_D*P_D'] vs. log t_D is 0.25.

$$\left(t_D * P_D'\right) = \frac{\pi}{4\sqrt{2C_{FD}}}\frac{t_D^{1/4}}{\Gamma(5/4)} \quad \text{(C.22)}$$

$$k_I = \left(\frac{14.132\, q_f B_o \mu_o}{\sqrt{\frac{2k_f w_f}{\bar{k}_I x_f}}\Gamma(5/4) h_I\,(t*\Delta P')}\left[\frac{t}{(\phi c)_{T_i}\,\mu x_f^2}\right]^{1/4}\right)^{1/0.75} \quad \text{(C.23)}$$

$$k_I = \left(\frac{142.521 q_f T}{\sqrt{\frac{2k_f w_f}{\bar{k}_I x_f}}\Gamma(5/4) h_I\left[t*\Delta(mP')\right]}\left[\frac{t}{(\phi c)_{T_i}\,\mu x_f^2}\right]^{1/4}\right)^{1/0.75} \quad \text{(C.24)}$$

For pressure,

$$P_{wD} = \frac{\pi}{\sqrt{2C_{FD}}}\frac{t_D^{1/4}}{\Gamma(5/4)} + s_c \quad \text{(C.25)}$$

If s_c=0

$$k_I = \left(\frac{56.5278\, q_f \beta_o \mu}{\sqrt{\frac{2k_f w_f}{\bar{k}_I x_f}}\Gamma(5/4) h_I\,\Delta P}\left[\frac{t}{(\phi c)_{T_i}\,\mu x_f^2}\right]^{1/4}\right)^{1/0.75} \quad \text{(C.26)}$$

$$k_I = \left(\frac{570.0821 q_f T}{\sqrt{\frac{2k_f w_f}{\bar{k}_I x_f}}\Gamma(5/4) h_I\,\Delta m(P)}\left[\frac{t}{(\phi c)_{T_i}\,\mu x_f^2}\right]^{1/4}\right)^{1/0.75} \quad \text{(C.27)}$$

The slope of straight line on log P_D vs. log t_D and log [t_D*P_D'] vs. log t_D is is (1/4).

$$\left(t_D * P_{wD}'\right) = \frac{\pi}{4\sqrt{2C_{FD}}}\frac{t_D^{1/4}}{\Gamma(5/4)\omega^{1/4}} \quad \text{(C.28)}$$

$$k_I = \left(\frac{14.132\, q_f B_o \mu_o}{\sqrt{\frac{2k_f w_f}{\bar{k}_I x_f}}\Gamma(5/4) h_I\,(t*\Delta P')}\left[\frac{t}{(\phi c)_{T_i}\,\mu x_f^2\omega}\right]^{1/4}\right)^{1/0.75} \quad \text{(C.29)}$$

$$k_I = \left(\frac{142.521 q_f T}{\sqrt{\frac{2k_f w_f}{\bar{k}_I x_f}}\Gamma(5/4) h_I\left[t*\Delta(mP')\right]}\left[\frac{t}{(\phi c)_{T_i}\,\mu x_f^2\omega}\right]^{1/4}\right)^{1/0.75} \quad \text{(C.30)}$$

For pressure,

$$P_{wD} = \frac{\pi}{\sqrt{2C_{FD}}}\frac{t_D^{1/4}}{\Gamma(5/4)\omega^{1/4}} + s_c \quad \text{(C.31)}$$

If s_c=0

$$k_I = \left(\frac{56.5278\, q_f B_o \mu_o}{\sqrt{\frac{2k_f w_f}{\bar{k}_I x_f}}\Gamma(5/4) h_I\,\Delta P}\left[\frac{t}{(\phi c)_{T_i}\,\mu x_f^2\omega}\right]^{1/4}\right)^{1/0.75} \quad \text{(C.32)}$$

$$k_I = \left(\frac{570.0821 q_f T}{\sqrt{\frac{2k_f w_f}{\bar{k}_I x_f}}\Gamma(5/4) h_I\,\Delta m(P)}\left[\frac{t}{(\phi c)_{T_i}\,\mu x_f^2\omega}\right]^{1/4}\right)^{1/0.75} \quad \text{(C.33)}$$

The slope of straight line on log P_D vs. log t_D and log [t_D*P_D'] vs. log t_D is 0.5.

$$\left(t_D * P_D'\right) = \frac{1}{2}\sqrt{\frac{\pi t_D}{\omega}} \quad \text{(C.34)}$$

$$k_I = \left(\frac{2.03205\, q_f B_o \mu_o}{h_I\,(t*\Delta P')}\sqrt{\frac{t}{(\phi c)_{T_i}\,\mu x_f^2\omega}}\right)^2 \quad \text{(C.35)}$$

$$k_I = \left(\frac{20.4932\, q_f T}{h_I\left[t*\Delta m(P)'\right]}\sqrt{\frac{t}{(\phi c)_{T_i}\,\mu x_f^2\omega}}\right)^2 \quad \text{(C.36)}$$

For pressure,

$$P_D = \sqrt{\frac{\pi t_D}{\omega}} + \frac{\pi}{3C_{FD}} + s_c \quad \text{(C.37)}$$

If s_c=0 and $C_{FD} \rightarrow \infty$,

$$k_I = \left(\frac{4.0641 q_f B_o \mu_o}{h_I \Delta P} \sqrt{\frac{t}{(\phi c)_{T_I} \mu x_f^2 \omega}} \right)^2 \quad \text{(C.38)}$$

$$k_I = \left(\frac{40.9864 q_f T}{h_I (\Delta m P)} \sqrt{\frac{t}{(\phi c)_{T_I} \mu x_f^2 \omega}} \right)^2 \quad \text{(C.39)}$$

The slope of straight line on log P_D vs. log t_D and log [t_D*P_D'] vs. log t_D is 0.5.

$$(t_D * P_D') = \frac{1}{2}\sqrt{\pi t_D} \quad \text{(C.40)}$$

$$k_I = \left(\frac{2.03205 q_f B_o \mu_o}{h_I (t * \Delta P')} \sqrt{\frac{t}{(\phi c)_{T_I} \mu x_f^2}} \right)^2 \quad \text{(C.41)}$$

$$k_I = \left(\frac{20.4932 q_f T}{h_I [t * \Delta (mP')]} \sqrt{\frac{t}{(\phi c)_{T_I} \mu x_f^2}} \right)^2 \quad \text{(C.42)}$$

For pressure,

$$P_D = \sqrt{\pi t_D} + \frac{\pi}{3C_{FD}} + s_c \quad \text{(C.43)}$$

If s_c=0 and $C_{FD} \rightarrow \infty$

$$k_I = \left(\frac{4.0641 q_f B_o \mu_o}{h_I \Delta P} \sqrt{\frac{t}{(\phi c)_{T_I} \mu x_f^2}} \right)^2 \quad \text{(C.44)}$$

$$k_I = \left(\frac{40.9864 q_f T}{h_I (\Delta m P)} \sqrt{\frac{t}{(\phi c)_{T_I} \mu x_f^2}} \right)^2 \quad \text{(C.45)}$$

C.3 Late time

The slope of straight line on log P_D vs. log t_D and log [t_D*P_D'] vs. log t_D is 1.

$$(t_D * P_D') = 2\pi t_{DA} \quad \text{(C.46)}$$

$$A = \frac{0.23395 q_f B_o}{(\phi c)_{T_I} h_I} \left(\frac{t}{(t * \Delta P')} \right) \quad \text{(C.47)}$$

$$A = \frac{2.3954 q_f T}{(\phi c)_{T_I} \mu h_I} \left(\frac{t}{[t * \Delta m(P)']} \right) \quad \text{(C.48)}$$

For pressure,

$$P_D = 2\pi t_{DA} + \frac{\pi y_{eD}}{6} + \frac{\pi}{3C_{FD}} + s_c \quad \text{(C.49)}$$

When $t_{DA} >> \frac{\pi y_{eD}}{12} + \frac{1}{6C_{FD}} + \frac{s_c}{2\pi}$

$$A = \frac{0.23395 q_f B_o}{(\phi c)_{T_I} h_I} \left(\frac{t}{\Delta P} \right) \quad \text{(C.50)}$$

$$A = \frac{2.3954 q_f T}{(\phi c)_{T_I} \mu h_I} \left(\frac{t}{\Delta m(P)} \right) \quad \text{(C.51)}$$

APPENDIX D. GOVERNING EQUATIONS FOR ASYMPTOTIC SOLUTIONS FOR PRESSURE AND DERIVATIVE: TRANSIENT DUAL-POROSITY MODEL

D.1 Early time

The slope of straight line on log P_D vs. log t_D and log [t_D*P_D'] vs. log t_D is is 1.

$$P_D = \frac{t_D}{C_D} \quad \text{(D.1)}$$

$$C = \frac{0.04167 q_f B_o h_t}{h_I} \frac{t}{\Delta P} \quad \text{(D.2)}$$

$$C = \frac{0.04167 q_f B_o h_t}{h_I} \frac{t}{(t * \Delta P')} \quad \text{(D.3)}$$

D.2 Intermediate time

The slope of straight line on log P_D vs. log t_D and log [t_D*P_D'] vs. log t_D is 1/8.

$$(t_D * P_D') = \left(\frac{3}{\lambda^9 \omega^9} \right)^{1/8} \frac{\pi}{8\sqrt{2C_{fD}}} \frac{t_D^{1/8}}{\Gamma(9/8)} \quad \text{(D.4)}$$

$$k_I = \left(\frac{19.7940 q_{f_o} B_o \mu_o}{h_I \sqrt{2\left(\frac{k_f w_f}{k_I x_f}\right)} \Gamma(9/8) (t * \Delta P')} \left(\frac{3t}{(\phi c_t) \mu_o x_f^2 \lambda^9 \omega^9} \right)^{1/8} \right)^{\frac{8}{7}} \quad \text{(D.5)}$$

$$k_I = \left(\frac{199.622 q_{f_g} T}{h_I \sqrt{2\left(\frac{k_f w_f}{k_I x_f}\right)} \Gamma(9/8) [t * \Delta m(P')]} \left(\frac{3t}{(\phi c_t)_{Ig} \mu_g x_f^2 \lambda^9 \omega^9} \right)^{1/8} \right)^{\frac{8}{7}} \quad \text{(D.6)}$$

For pressure,

$$P_D = \left(\frac{3}{\lambda^9\omega^9}\right)^{1/8} \frac{\pi}{\sqrt{2C_{fD}}} \frac{t_D^{1/8}}{\Gamma(9/8)} + Sc \quad (D.7)$$

If s_c=0

$$k_I = \left(\frac{158.3519 q_{f_o} B_o \mu_o}{h_I \sqrt{2\left(\frac{k_f w_f}{\bar{k}_I x_f}\right)}\, \Gamma(9/8)\,(\Delta P)} \left(\frac{3t}{(\phi c_t)\mu_o x_f^2 \lambda^9 \omega^9} \right)^{1/8} \right)^{\frac{8}{7}} \quad (D.8)$$

$$k_I = \left(\frac{1596.98 q_{f_g} T}{h_I \sqrt{2\left(\frac{k_f w_f}{\bar{k}_I x_f}\right)}\, \Gamma(9/8)\,\Delta m(P)} \left(\frac{3t}{(\phi c_t)_{Ig} \mu_g x_f^2 \lambda^9 \omega^9} \right)^{1/8} \right)^{\frac{8}{7}} \quad (D.9)$$

The slope of straight line on log P_D vs. log t_D and log [t_D*P_D'] vs. log t_D is 0.25.

$$\left(t_D * P_D'\right) = \frac{\pi}{4\sqrt{2C_{fD}}} \frac{t_D^{1/4}}{\Gamma(5/4)} \quad (D.10)$$

$$k_I = \left(\frac{14.1319 q_{f_o}}{h_I \sqrt{2\left(\frac{k_f w_f}{\bar{k}_I x_f}\right)}\, \Gamma(5/4)\,(t * \Delta P')} \left(\frac{t}{(\phi c_t)\mu_o x_f^2} \right)^{1/4} \right)^{\frac{1}{0.75}} \quad (D.11)$$

$$k_I = \left(\frac{142.5205 q_{f_g} T}{h_I \sqrt{2\left(\frac{k_f w_f}{\bar{k}_I x_f}\right)}\, \Gamma(5/4)\left[t * \Delta(mP')\right]} \left(\frac{3t}{(\phi c_t)_{Ig} \mu_g x_f^2} \right)^{1/4} \right)^{\frac{1}{0.75}} \quad (D.12)$$

For pressure,

$$P_{wD} = \frac{\pi}{\sqrt{2C_{fD}}} \frac{t_D^{1/4}}{\Gamma(5/4)} + Sc \quad (D.13)$$

If s_c=0

$$k_I = \left(\frac{56.5278 q_{f_o} B_o \mu_o}{h_I \sqrt{2\left(\frac{k_f w_f}{\bar{k}_I x_f}\right)}\, \Gamma(5/4)\,(\Delta P)} \left(\frac{t}{(\phi c_t)\mu_o x_f^2} \right)^{1/4} \right)^{\frac{1}{0.75}} \quad (D.14)$$

$$k_I = \left(\frac{570.0820 q_{f_g} T}{h_I \sqrt{2\left(\frac{k_f w_f}{\bar{k}_I x_f}\right)}\, \Gamma(5/4)\,(\Delta mP)} \left(\frac{t}{(\phi c_t)_{Ig} \mu_g x_f^2} \right)^{1/4} \right)^{\frac{1}{0.75}} \quad (D.15)$$

The slope of straight line on log P_D vs. log t_D and log [t_D*P_D'] vs. log t_D is 0.25.

$$\left(t_D * P_{wD}'\right) = \frac{\pi}{4\sqrt{2C_{fD}}} \frac{t_D^{1/4}}{\Gamma(5/4)\,(1+\omega)^{1/4}} \quad (D.16)$$

$$k_I = \left(\frac{14.1319 q_{f_o} B_o \mu_o}{h_I \sqrt{2\left(\frac{k_f w_f}{\bar{k}_I x_f}\right)}\, \Gamma(5/4)\,(t * \Delta P')} \left(\frac{t}{(\phi c_t)\mu_o x_f^2 (1+\omega)} \right)^{1/4} \right)^{\frac{1}{0.75}} \quad (D.17)$$

$$k_I = \left(\frac{142.5205 q_{f_g} T}{h_I \sqrt{2\left(\frac{k_f w_f}{\bar{k}_I x_f}\right)}\, \Gamma(5/4)\left[t * \Delta(mP')\right]} \left(\frac{t}{(\phi c_t)_{Ig} \mu_g x_f^2\,(1+\omega)} \right)^{1/4} \right)^{\frac{1}{0.75}} \quad (D.18)$$

For pressure,

$$P_D = \frac{\pi}{\sqrt{2C_{fD}}} \frac{t_D^{1/4}}{\Gamma(5/4)\,(1+\omega)^{1/4}} + Sc \quad (D.19)$$

If s_c=0,

$$k_I = \left(\frac{56.5278 q_{f_o} B_o \mu_o}{h_I \sqrt{2\left(\frac{k_f w_f}{\bar{k}_I x_f}\right)}\, \Gamma(5/4)\,(\Delta P)} \left(\frac{t}{(\phi c_t)\mu_o x_f^2\,(1+\omega)} \right)^{1/4} \right)^{\frac{1}{0.75}} \quad (D.20)$$

$$k_I = \left(\frac{570.0820\, q_{f_g}\, T}{h_I \sqrt{2\left(\frac{k_f w_f}{\bar{k}_I\, x_f}\right)}\, \Gamma(5/4)\, \Delta m(P)} \left(\frac{t}{(\phi c_t)_{Ig}\, \mu_g\, x_f^2\, (1+\omega)} \right)^{1/4} \right)^{\frac{1}{0.75}} \quad \text{(D.21)}$$

The slope of straight line on log P_D vs. log t_D and log [t_D*P_D'] vs. log t_D is 0.25, and if s_c →0 and C_{fD} →∞

$$\left(t_D * P_D'\right) = \frac{\pi}{8\Gamma(5/4)} \left(\frac{3t_D}{\lambda\omega} \right)^{1/4} \quad \text{(D.22)}$$

$$k_I = \left(\frac{7.066\, q_{f_o}\, B_o \mu_o}{h_I\, \Gamma(5/4)\, (t * \Delta P')} \left(\frac{3t}{(\phi c_t)\mu_o\, x_f^2\, (\omega\lambda)} \right)^{1/4} \right)^{\frac{1}{0.75}} \quad \text{(D.23)}$$

$$k_I = \left(\frac{71.2603\, q_{f_g}\, T}{h_I\, \Gamma(5/4) \left[t * \Delta m(P')\right]} \left(\frac{3t}{(\phi c_t)_{Ig}\, \mu_g\, x_f^2\, (\omega\lambda)} \right)^{1/4} \right)^{\frac{1}{0.75}} \quad \text{(D.24)}$$

For pressure,

$$P_D = \frac{\pi}{2\Gamma(5/4)} \left(\frac{3t_D}{(\lambda\omega)} \right)^{1/4} + \frac{\pi}{3C_{fD}} + Sc \quad \text{(D.25)}$$

If s_c=0 and C_{fD} →∞ $\frac{\pi}{3\, C_{fD}} \to 0$

$$k_I = \left(\frac{28.2639\, q_{f_o}\, B_o \mu_o}{h_I\, \Gamma(5/4)\, (\Delta P)} \left(\frac{3t}{(\phi c_t)\mu_o\, x_f^2\, (\lambda\omega)} \right)^{1/4} \right)^{\frac{1}{0.75}} \quad \text{(D.26)}$$

$$k_I = \left(\frac{285.041 q_{f_g}\, T}{h_I\, \Gamma(5/4)\, (\Delta m P)} \left(\frac{3t}{(\phi c_t)_{Ig}\, \mu_g\, x_f^2\, (\lambda\omega)} \right)^{1/4} \right)^{\frac{1}{0.75}} \quad \text{(D.27)}$$

The slope of straight line on log P_D vs. log t_D and log [t_D*P_D'] vs. log t_D is 0.5, and if s_c →0 and C_{fD} →∞

$$\left(t_D * P_D'\right) = \frac{1}{2}\sqrt{\pi\, t_D} \quad \text{(D.28)}$$

$$k_I = \left(\frac{2.032\, q_{f_o}\, B_o \mu_o}{h_I\, (t * \Delta P')} \left(\frac{t}{(\phi c_t)\mu_o\, x_f^2} \right)^{1/2} \right)^2 \quad \text{(D.29)}$$

$$k_I = \left(\frac{20.4932\, q_{f_g}\, T}{h_I\, \left[t * \Delta m(P)'\right]} \left(\frac{t}{(\phi c_t)_{Ig}\, \mu_g\, x_f^2} \right)^{1/2} \right)^2 \quad \text{(D.30)}$$

For pressure,

$$P_D = \sqrt{\pi t_D} + \frac{\pi}{3C_{fD}} + Sc \quad \text{(D.31)}$$

If s_c=0 and C_{fD} →∞ $\frac{\pi}{3\, C_{fD}} \to 0$

$$k_I = \left(\frac{4.0641\, q_{f_o}\, B_o \mu_o}{h_I\, (\Delta P)} \left(\frac{t}{(\phi c_t)\mu_o\, x_f^2} \right)^{1/2} \right)^2 \quad \text{(D.32)}$$

$$k_I = \left(\frac{40.9864\, q_{f_g}\, T}{h_I\ \Delta m(P)} \left(\frac{t}{(\phi c_t)_{Ig}\, \mu_g\, x_f^2} \right)^{1/2} \right)^2 \quad \text{(D.33)}$$

The slope of straight line on log P_D vs. log t_D and log [t_D*P_D'] vs. log t_D is 0.5,

$$\left(t_D * P_D'\right) = \frac{1}{2\, y_{eD}} \sqrt{\frac{3\pi\, t_D}{\lambda\omega}} \quad \text{(D.34)}$$

$$k_I = \left(\frac{3.5196\, q_{f_o}\, B_o \mu_o}{h_I\, y_e\, (t * \Delta P')} \left(\frac{t}{(\phi c_t)\mu_o\, (\lambda\omega)} \right)^{1/2} \right)^2 \quad \text{(D.35)}$$

$$k_I = \left(\frac{35.4953\, q_{f_g}\, T}{h_I\ y_e \left[t * \Delta (mP')\right]} \left(\frac{t}{(\phi c_t)_{Ig}\, \mu_g\, (\lambda\omega)} \right)^{1/2} \right)^2 \quad \text{(D.36)}$$

For pressure,

$$P_D = \frac{1}{y_{eD}} \sqrt{\frac{3\pi t_D}{\lambda\, \omega}} + \frac{\pi\, y_{eD}}{6} + \frac{\pi}{3C_{fD}} + Sc \quad \text{(D.37)}$$

If s_c=0

$$\Delta P = \frac{141.2\, q_f\ \beta\, \mu}{k_I h_I} \left[0.08635 \frac{x_f}{y_e} \sqrt{\frac{k_I t}{\lambda\, \omega}} + \frac{\pi\, y_e}{6 x_f} + \frac{\pi}{3\sqrt{\frac{2k_f w_f}{\bar{k}_I\, x_f}}} \right] \quad \text{(D.38)}$$

$$\Delta m P = \frac{1424\, q_{fg}\, T}{k_I h_I} \left[0.08635 \frac{x_f}{y_e} \sqrt{\frac{k_I t}{\lambda\, \omega}} + \frac{\pi\, y_e}{6 x_f} + \frac{\pi}{3\sqrt{\frac{2k_f w_f}{\bar{k}_I\, x_f}}} \right] \quad \text{(D.39)}$$

The slope of straight line on log P_D vs. log t_D and log [t_D*P_D'] vs. log t_D is 0.5, and if s_c →0 and C_{fD} →∞

$$\left(t_D * P_D'\right) = \frac{1}{2}\sqrt{\frac{\pi\, t_D}{(1+\omega)}} \quad \text{(D.40)}$$

$$k_I = \left(\frac{2.032\, q_{f_o} B_o \mu_o}{h_I\ (t * \Delta P')}\left(\frac{t}{(\phi c_t)\mu_o (1+\omega)}\right)^{1/2}\right)^2 \quad \text{(D.41)}$$

$$k_I = \left(\frac{20.4932\ q_{f_g} T}{h_I\ \left[t * \Delta(mP')\right]}\left(\frac{t}{(\phi c_t)_{Ig}\mu_g (1+\omega)}\right)^{1/2}\right)^2 \quad \text{(D.42)}$$

For pressure,

$$P_D = \sqrt{\frac{\pi t_D}{(1+\omega)}} + \frac{\pi}{3C_{fD}} + Sc \quad \text{(D.43)}$$

If s_c=0 and $C_{fD} \rightarrow \infty$ $\frac{\pi}{3\,C_{fD}} \rightarrow 0$

$$k_I = \left(\frac{4.0641 q_{f_o} B_o \mu_o}{h_I\ \Delta P}\left(\frac{t}{(\phi c_t)\mu_o (1+\omega)}\right)^{1/2}\right)^2 \quad \text{(D.44)}$$

$$k_I = \left(\frac{40.9864\ q_{f_g} T}{h_I\ \ (\Delta mP)}\left(\frac{t}{(\phi c_t)_{Ig}\mu_g (1+\omega)}\right)^{1/2}\right)^2 \quad \text{(D.45)}$$

D.3. Late time

The slope of straight line on log P_D vs. log t_D and log [t_D*P_D'] vs. log t_D is 1.

$$\left(t_D * P_D'\right) = \frac{2\pi t_{DA}}{1+\omega} \quad \text{(D.46)}$$

$$A = \frac{0.23395\, q_f B_o}{(\phi c)_{T_I}\ h_I (1+\omega)}\left(\frac{t}{(t * \Delta P')}\right) \quad \text{(D.47)}$$

$$A = \frac{2.3594\, q_{fg} T}{(\phi c)_{T_I}\ \mu_g h_I (1+\omega)}\left(\frac{t}{\left[t * \Delta m(P)'\right]}\right) \quad \text{(D.48)}$$

For pressure,

$$P_D = \frac{2\pi t_{AD}}{1+\omega} + \frac{\pi y_{eD}}{6} + \frac{\pi}{3C_{FD}} + s_c \quad \text{(D.49)}$$

When $t_{DA} >> \frac{\pi y_{eD}}{12} + \frac{1}{6C_{FD}} + \frac{s_c}{2\pi}$

$$A = \frac{0.23395\, q_f B_o}{(\phi c)_{T_I}\ h_I (1+\omega)}\left(\frac{t}{\Delta P}\right) \quad \text{(D.50)}$$

$$A = \frac{2.3594\, q_f T}{(\phi c)_{T_I}\ \mu h_I\ (1+\omega)}\left(\frac{t}{\Delta m(P)}\right) \quad \text{(D.51)}$$

Nomenclature

A	Drainage area, ft^2
B_o	Volumetric factor, bbl/STB
c_t	System total compressibility, 1/psi
c_{tO}	Total compressibility of the inner reservoir,1/psi
c_{tI}	Total compressibility of the outer reservoir, 1/psi
c_{tf}	Total hydraulic compressibility, 1/psi
c	Wellbore-storage coeffi cient, bbl/psi
C_D	Dimensionless wellbore-storage coefficient
h	Reservoir thickness, ft
k_I	Permeability of the inner reservoir, md
k_o	Permeability of the outer reservoir, md
k_f	Hydraulic-fracture permeability, md
n_f	Number of main fracture planes
P_i	Initial reservoir Pressure, psi
$\overline{P}$	Laplace-space pressure
P_{wf}	Bottomhole flowing pressure, psi
$\overline{q}$	Laplace-space flow rate
q	production rate, STB/D, Mscf/D
r_w	wellbore radius, ft
t	Time, hr
t_D	Dimensionless time
$t*m(P)'$	Pseudopressure derivative, psi^2/cp
$t*\Delta P'$	Pressure derivative, psi
T	Absolute Temperature, °R
w_f	Hydraulic-fracture width, ft
u	Laplace space variable
x_e	effective reservoir width, ft
x_f	Hydraulic half-fracture length, ft
x_{eD}	Dimensionless reservoir size in x-direction.
y_{eD}	Dimensionless reservoir size in y-direction.
α_f	Hydraulic-fracture parameter used in trilinear-flow model
α_O	Outer-reservoir parameter used in trilinear-flow model
β_F	hydraulic-fracture parameter used in trilinear-flow model
β_O	Outer-reservoir parameter used in trilinear-flow model
η_f	Hydraulic-fracture diffusivity, ft^2/hr
η_I	Inner-reservoir diffusivity, ft^2/hr
η_o	Outer-reservoir diffusivity, ft2/hr
η_{fD}	Hydraulic-fracture-diffusivity ratio
η_{oD}	Outer-reservoir diffusivity ratio
λ	Flow-capacity ratio
ω	Storativity ratio

Greeks

ϕ	Porosity, fraction
μ	Viscosity, cp

Suffices

o	Crudo
i	Initial
D	Dimensionless
DA	Dimensionless based on drainage area
BL	Bilinear
L	Linear
PSS	Pseudosteady state
sc	Standard conditions
TL	Trilinear
qPSS	First pseudosteady state regime